Modelling collision outcome in moderately dense sprays

Gautier Luret, Thibaut Menard, Gregory Blokkeel, Alain Berlemont, Julien Reveillon, François-Xavier Demoulin

Submitted to International Journal of Atomization and Spray as a full length paper, selected among ILASS–Europe 2008 conference papers

Modelling collision outcome in moderately dense sprays

Gautier LURET, Thibaut MENARD, Grégory BLOKKEEL, Alain BERLEMONT, Julien REVEILLON and François-Xavier DEMOULIN

Gautier LURET, Thibaut MENARD, Alain BERLEMONT, Julien REVEILLON, François-Xavier DEMOULIN

Coria UMR6614 CNRS
Université de Rouen
BP 12, Site universitaire du Madrillet
76801 Saint Etienne du Rouvray Cedex, France

Grégory BLOKKEEL

PSA Peugeot Citroën.
Route de Gisy
78943 Vélizy-Villacoublay Cedex, France

Author correspondence :

François-Xavier DEMOULIN
Coria UMR6614 CNRS
Université de Rouen
BP 12, Site universitaire du Madrillet
76801 Saint Etienne du Rouvray Cedex, France
Tel : 00 33 2 32 95 36 74
Fax : 00 33 2 32 91 04 85
E-mail : demoulin@coria.fr

Abstract

To simulate primary atomization, the dense zone of sprays has to be addressed and new atomization models have been developed as the ELSA model [4]. A transport equation for the liquid/gas interface density is stated and extends the concept of droplet diameter. Several related source terms require modelling attention. This work describes the contribution of collision and coalescence processes. Several questions arise: Is it possible to represent collision/coalescence from an Eulerian description of the flow? What are the key parameters? What are the particular features of collision in dense spray? To answer these questions, a Lagrangian test case, carefully resolved statistically, is used as a basis to evaluate Eulerian models. It is shown that a significant parameter is the equilibrium Weber number: If it is known, Eulerian models are able to reproduce the main features of Lagrangian simulations. To overcome the Lagrangian collision model simplification that mostly considers collisions between spherical droplets, a new test case has been designed to focus on collision process in dense spray. The numerical code, Archer, which is developed to handle interface behaviours in two-phase flow by the way of direct numerical simulation (DNS) [19] is used. Thanks to DNS simulations and experimental observations, the importance of non spherical collisions is demonstrated. Despite some classical drawbacks of DNS, we observed that an equilibrium Weber number can be determined in the considered test case. This work emphasizes the ability of interface DNS simulations to describe complex turbulent two phase flows with interfaces and to stand as a complement to new experiments.

1 Introduction

Energy and environment survey are becoming public policy issues, such as greenhouse effects and global warming. As a consequence, drastic limitations of emissions are imposed to the automotive industry. The European car manufacturers will be subjected to more stringent emissions regulation (such as Euro 5 and post-Euro 5 standards), concerning nitrogen oxides (Nox), CO2, unburned hydrocarbons (HC) and particle emissions. To reach these tolerance thresholds, the automotive research is looking for multiple processes that are involved in combustion: fuel distribution (injection), internal aerodynamics (vaporization, mixing) and combustion itself (ignition, chemical reactions).

For many decades, great attention has been devoted to the injection process. It is a determining factor for the fuel distribution inside the combustion chamber, and it contributes indirectly to the pollutants formation. Its optimization may notably lead to a cleaner Internal Combustion Engine (ICE). For instance, following the injector nozzle geometry [1] and the injection strategy [2, 3], the overall spray behaviour and its characteristics may be drastically different. The liquid jet atomization has thus to be well-understood, but unfortunately several complex mechanisms are involved, such as turbulence, primary and secondary breakup, droplet collision and coalescence. All these mechanisms have to be taken into account to determine the spray dispersion and the local droplet diameter and velocity distributions. From a correct modelling of the injection and atomization process it is then possible to compute in a realistic way the droplet-vaporisation, vapour mixing and combustion processes [4].

Furthermore, one characteristic of high-pressure Diesel jets is the presence of a liquid core which is attached to the exit of the nozzle. This part of the jet and its vicinity are more commonly called the dense zone. It is the most difficult zone to model partly because of the lack of experimental data despite recent advances in optical techniques [5-7]. However it is

obvious that a realistic description of the dense part improves significantly the global modelling of the injection [4, 8-10]. To deal with the dense part, Lebas et *al.* [4] extended the Eulerian Lagrangian Spray Atomization (ELSA) model (originally proposed by [11]) to Diesel injection. The model is based on a single-phase Eulerian description of the flow that is composed of a liquid and a gas mixture. The initial dispersion and atomization of the liquid jet are assumed to be dominated by the turbulence, but by taking into account for high variable density [12]. A transport equation for the mean liquid/gas interface density is also considered to describe the complex liquid topology. Indeed, in the initial part of the jet, the notion of droplet diameter is not applicable, as no droplet is formed yet. Thus the quantity of interface is a first order parameter that can help in describing the different interactions between the liquid and the gas phases.

The surface density is a particular variable because it can be defined locally only by using generalized functions. This is a Dirac function. Nevertheless, the local equation can be determined, see for instance a review on this problem by Morel [13]. But the link has not yet been established with modeled equations that are currently used for RANS (Reynolds Average Navier Stokes) simulations [4, 11, 14] or LES (Large Eddy Simulation) simulations [15] . Among the processes that play a role on the surface density, the effect of collision/coalescence is expected to be significant especially because we deal with the dense zone of the spray. Different terms in the currently used equations are assumed to take the collision/coalescence effects into account. But it remains obvious that extended researches on this topic are still required.

The first question concerns the dispersed phase in the resulting spray and the ability of Eulerian methods to represent collision/coalescence phenomena. Indeed by comparisons with Lagrangian methods that totally describe the PDF (probability density function) of the spray, the Eulerian approaches are generally using only few moments of the distribution to describe

the whole PDF. As a consequence, information can be lost, depending on the assumed shape of the PDF, that can only be built with the retained moments. The collision process describes how two or more droplets interact when their respective motion induces crossing trajectories. It is obvious that characteristics of each colliding droplet are important to determine the regime of the collision, see for instance [16]. Clearly, knowing the outcome of each individual collision is not among the capability of Eulerian methods but this is not necessary. The expected behaviour of the collision/coalescence model for an Eulerian method is to predict correctly the effect of the whole set of collision on the retained statistical moments used to describe the spray. Considering the Eulerian methods currently used to describe the atomization, this property will be studied as far as the mean surface density is concerned. To do so, a test case, well resolved from a statistical point of view using Lagrangian models of collision/coalescence, is proposed.

The second problem concerns the validity of the collision/coalescence models currently used to compute the evolution of the mean (or filtered) surface density in the dense zone. Indeed, the first class of models proposed by Vallet et al. [11, 17] and then by Iyer and Abraham [18] are based on droplet collisions. Therefore, these models are applied in the dense part of the spray where the droplets are not formed yet! A global model proposed specifically for the dense part of the spray has been proposed by Lebas et al. [4]. Although, this model participates to the correct behaviour of the computed spray, it has not been proved to behave properly as far as the collision/coalescence processes are concerned. Moreover it has been outlined [4] that some of its parameters have still to be established. Collision has been studied experimentally only for droplet collision, conditions that are far to those encountered in the dense part of the spray. To design and to characterise an experiment of collision between two non spherical parcels of liquid is not an obvious task. Consequently to understand collisions in the dense zone, a numerical test case has been put forward thanks to the Archer code that

has been developed to compute two-phase flow by the way of direct numerical simulation (DNS) [19]. These simulations are still difficult and computationally expensive, thus, preliminary results are presented here. They concern few cases representative of what can be encountered during an atomization process.

This article is organized as follow: In the first part the Eulerian approach ELSA used to compute the atomization is described. Then a Lagrangian simulation is put forward to determine the ability of the Eulerian approach to represent the collision/coalescence phenomena. The third part of this paper describes a direct numerical simulation used to study collision and coalescence of non spherical liquid parcel.

2 THE EULERIAN-LAGRANGIAN SPRAY ATOMIZATION MODEL

In this section the ELSA model is described to understand where the collision/coalescence effects are expected to play a role in the complete formulation. The goal of the ELSA model is to describe realistically the dense zone of the spray. Based on the assumption that the Weber and Reynolds numbers have to be high, the ELSA model is naturally well adapted to Diesel Direct Injection conditions. This assumption corresponds to an initial atomization dominated by aerodynamic forces. The global behaviour of the model and its ability to describe Diesel injection have been checked out by Lebas et al. [4].

A liquid-gas flow is considered as a unique flow with a highly variable density $\overline{\rho}$ which can be determined thanks to the following equation:

$$\frac{1}{\overline{\rho}} = \frac{\widetilde{Y}_l}{\rho_l} + \frac{1-\widetilde{Y}_l}{\rho_g} \qquad (1)$$

$\tilde{Y}_l$ corresponds to the mean liquid mass fraction. While, ρ_g and ρ_l are respectively the gas and the liquid densities. ρ_g follows the state equation of a perfect gas (by taking the liquid

volume fraction into account) and ρ_l account for the fact that the liquid density can be modified accordingly to the liquid temperature.

Considering the two-phase flow as a unique mixture flow with a highly variable density implies that the transport equation for the mean velocity does not contain any momentum exchange terms between the liquid and the gas phases. Additionally, under the assumption of high values of both Reynolds and Weber numbers, laminar viscosity and surface tension forces can be neglected:

$$\frac{\partial \overline{\rho}\widetilde{u}_i}{\partial t} + \frac{\partial \overline{\rho}\widetilde{u}_i\widetilde{u}_j}{\partial x_j} = -\frac{\partial \overline{P}}{\partial x_i} - \frac{\partial \overline{\rho}\,\widetilde{u_i''u_j''}}{\partial x_i} \tag{2}$$

This “mixture” approach has to be combined with a turbulence model. The (*k*-ε) model is generally used even if other models have been tested [12]. The Boussinesq hypothesis is chosen to model the Reynolds stress tensor.

A regular transport equation stands for the mean liquid mass fraction $\tilde{Y}_l$ with a source term representing the effect of vaporization:

$$\frac{\partial \overline{\rho}\widetilde{Y}_l}{\partial t} + \frac{\partial \overline{\rho}\widetilde{Y}_l\widetilde{u}_i}{\partial x_i} = \frac{\partial}{\partial x_j}\left(\frac{\mu_t}{Sc_{t,l}}\frac{\partial \widetilde{Y}_l}{\partial x_j}\right) - \overline{\rho}\dot{m}_{v,ELSA}\widetilde{\Omega} \tag{3}$$

$\widetilde{\Omega}$ is the liquid-gas interface density per unit of mass and $\dot{m}_{v,ELSA}$ represents the vaporization rate per unit of mass. It has been modeled from Abramzon and Sirignano’s approach [20, 21].

To determine the amount of surface between the two phases, classical approaches consist in considering spherical liquid drops and than using the diameter as geometrical parameter. But a more general parameter has to be used where a diameter of droplet cannot be defined: the

liquid-gas interface density, noted $\overline{\Sigma}$ when expressed per unit of volume or $\widetilde{\Omega}$ when given per unit of mass. The following equation relates both definitions:

$$\overline{\rho}\widetilde{\Omega} = \overline{\Sigma} \tag{5}$$

The transport equation for this variable is postulated. In the latest version of the ELSA model, it takes the following form [4]:

$$\frac{\partial \overline{\rho}\widetilde{\Omega}}{\partial t} + \frac{\partial \overline{\rho}\widetilde{u}_j\widetilde{\Omega}}{\partial x_j} = \frac{\partial}{\partial x_j}\left(\frac{\mu_t}{Sc_{t,\Omega}}\frac{\partial \widetilde{\Omega}}{\partial x_j}\right) + \Psi\left(\phi_{init.} + \phi_{turb.}\right) + \left(1-\Psi\right)\left(\phi_{coll./coal.} + \phi_{2ndBU} + \phi_{vapo.}\right) \tag{6}$$

This equation must be applicable from the dense zone up to the dispersed spray where droplets are eventually formed. In this latter case, an equivalent diameter of Sauter can be defined using the liquid-gas interface density and the mean liquid mass fraction :

$$D_{32} = \frac{6\widetilde{Y}_l}{\rho_l\widetilde{\Omega}} \tag{7}$$

Each source term ϕ_i (equation 4) models a specific physical phenomenon encountered by the liquid blobs or droplets. Lets

$$\phi_{init.} = \frac{12\overline{\rho}\mu_t}{\rho_l\rho_g Sc_t L_t}\frac{\partial \widetilde{Y}_l}{\partial x_i}\frac{\partial \widetilde{Y}_l}{\partial x_i} \tag{8}$$

be an initialization term, taking high values near the injector nozzle, where the mass fraction gradients take its highest values. It corresponds to the minimum production of liquid-gas interface density necessarily induced by the mixing between the liquid and gas phases, see Beau and Demoulin [22].

$$\phi_{turb.} = \frac{\overline{\rho}\widetilde{\Omega}}{\tau_t}\left(1-\frac{\widetilde{\Omega}}{\widetilde{\Omega}_1^*}\right) \tag{9}$$

$\phi_{turb.}$ corresponds to the production/destruction of liquid gas interface density due to the turbulent flow stretching and the effects of collision and coalescence in the dense part of the spray. It is supposed to be driven by a turbulent time scale τ_t. This production/destruction term is defined to reach an equilibrium liquid-gas interface density $\tilde{\Omega}_1^*$. It corresponds to the quantity of surface obtained at equilibrium under given flow conditions. Several formulations can be proposed. In Lebas et al. [4], an equilibrium Weber number is supposed: $We_1^* = 1$:

$$\tilde{\Omega}_1^* = \frac{\bar{\rho}\tilde{k}\tilde{Y}_l}{\rho_l \sigma_l We_1^*} \tag{10}$$

Where σ_l is the surface tension of the liquid phase.

$\phi_{coll./coal.}$ models the production/destruction of liquid-gas interface density due to the effects of collision and coalescence in the dilute spray region. Different proposals will be discussed extensively in the next section of this article.

$$\phi_{2ndBU} = Max\left[\frac{\bar{\rho}\tilde{\Omega}}{\tau_{2ndBU}}\left(1-\frac{\tilde{\Omega}}{\tilde{\Omega}_3^*}\right);0\right] \tag{11}$$

ϕ_{2ndBU} deals with the production of liquid-gas interface density due to the effects of secondary breakup in the dilute spray region. This source term is derived from the work of Pilch and Erdman [23]. It enables the estimation of the breakup time scale τ_{2ndBU} accordingly to the Weber number of the gas phase We_g, thanks to empirical correlations. Moreover, it determines the stable Weber number We_3^* with:

$$We_3^* = 12\left(1+1.077Oh^{1.6}\right) \tag{12}$$

Oh is the Ohnesorge number. The stable interface density that corresponds to stable droplets as far as the secondary breakup is concerned, written as follow:

$$\tilde{\Omega}_{crit,3} = \frac{6\rho_l u_{rel}^2 \tilde{Y}_l}{\rho_l \sigma_l We_{crit,3}} \tag{13}$$

with u_{rel} the relative velocity between the liquid and gas phases. Vaporisation is characterized thanks to:

$$\phi_{vapo} = -\frac{2}{3}\frac{\overline{\rho}\tilde{\Omega}^2}{\tilde{Y}_l}\dot{m}_{v,ELSA} \tag{14}$$

$\phi_{vapo.}$ comes from a classical adaptation of the "D^2" law of vaporization models for droplets and deals with the effects of destruction of liquid-gas interface density due to vaporization.

The transport equation of $\tilde{\Omega}$ takes into account several physical phenomena encountered by the liquid phase. Some of them are specifically observed in the dense zone of the spray and other are dedicated to dispersed spray regions. A function Ψ has been introduced to switch from the dense formulation to the dispersed formulation continuously and linearly in term of liquid volume fraction [4]. The transition zone is determined by two volume fraction limit values: $\phi_{dense} = 0.5$ and $\phi_{dilute} = 0.1$. The liquid volume fraction ϕ_l can be obtained thanks to the following relation:

$$\phi_l = \frac{\overline{\rho}\tilde{Y}_l}{\rho_l} \tag{15}$$

This description of the ELSA model show how an Eulerian method can be derived to deal with atomisation. Though it has been shown [4] that the presented form of the model is able to capture the global features of the atomisation of a Diesel jet, more detailed studies are still required. Indeed, to validate the various source terms of the surface density equation, specific studies for each kind of phenomena are required. In the following, test cases are put forward to study the particular effect of collisions. This phenomenon is expected to be important for a model devoted to the dense zone of a spray.

3 Variation of surface by collision in Eulerian approaches

Two types of processes due to collision can substantially modify the liquid-gas interface density with particularly opposite effects on its development.

On the one hand, coalescence decreases the surface density. Indeed, when two droplets merge into one, the surface area between the liquid and gas phases decreases. On the other hand, the collision-induced break-up plays the role of a production term and it has obviously a reverse effect. Several satellite droplets, produced after collision, represent a more important surface area than their parent droplets. Consequently, if flow conditions are kept statistically stationary, an equilibrium state is reached. It can be characterized thanks to a mean equilibrium surface density $\tilde{\Omega}^*$, which is related to an equilibrium Sauter mean diameter D_{32}^* (Eq. (7)) and an equilibrium Weber number of collision, We^*:

$$We^* = We_{coll}\left(D_{32}^*\right) = \frac{\rho_l u_l^2 D_{32}^*}{\sigma_l}, \tag{16}$$

where u_l is the liquid velocity fluctuation. *Note that the equilibrium Weber number of collision represents the ratio between liquid kinetic energy of agitation and the surface energy of the spray. It is different of the collision Weber number used to characterize each collision between two droplets.* This equilibrium state characterizes the asymptotic behaviour of a spray that experiences collision processes. Nevertheless, to properly describe these processes, it is necessary to predict the behaviour of the spray up to its equilibrium state. From an Eulerian point of view, several formulations of the collision source terms in liquid surface density equation have been proposed .

Iyer and Abraham [14] derived an expression adapted from a Lagrangian approach, initially developed by O'Rourke and Bracco [24] and based on the collision frequency between liquid droplets:

$$f_{coll} = \frac{N_d}{\tau_{coll}} = N_d^2 \, u_l \, \frac{\pi D_d^2}{2} \tag{17}$$

Where, u_l is an approximation of the relative velocity between the droplets. It depends on the liquid kinetic energy:

$$u_l = C_{col}\sqrt{\frac{2k_l}{3}} \tag{18}$$

The decrease rate of the number density due to the coalescence depends on a coalescence probability or coalescence efficiency η_{coll} derived from Brazier-Smith *et al.*'s correlation [25], which can be written as:

$$\frac{dN_d}{dt} = -\eta_{coll} f_{coll} \tag{19}$$

With,

$$\eta_{coll} = \min\left(\frac{6.24}{We_{coll}};1\right) \tag{20}$$

The collision source term derived for the surface density equation, Eq.(6), has been adapted from the Lagrangian formulation and retained by Iyer and Abraham [14]. It is given by:

$$\phi_{coll./coal.} = \phi_{coal} = -\eta_{coll}\overline{\rho}\,\widetilde{\Omega}^2\,\frac{u_l}{12} \tag{21}$$

Unfortunately, Iyer and Abraham did not propose any source term concerning the collision-induced breakup, even if other source terms counterbalance the coalescence in their case. Source terms are due to aerodynamic breakup and to vaporization. But if collisions are considered on their own, the diameter will diverge inexorably towards an infinite value (see Fig. 1). This model is referred as "Iyer" in the following.

Within the ELSA framework presented previously Beau and Demoulin [22] have suggested one source term for each process (coalescence and collision-induced breakup) as did Vallet *et al.* [11]:

$$\begin{cases} \phi_{coal} = -\dfrac{\overline{\rho}}{\tau_{coll}} \dfrac{\widetilde{\Omega}^2}{\Omega^{*}{}_2} \\ \phi_{bup} = \dfrac{\overline{\rho}\widetilde{\Omega}}{\tau_{coll}} \end{cases} \Rightarrow \phi_{coll/coal} = \frac{\overline{\rho}\widetilde{\Omega}}{\tau_{coll}} \left(1 - \frac{\widetilde{\Omega}}{\Omega^{*}{}_2} \right) \tag{22}$$

The form of the characteristic collision time scale τ_{coll} is similar to Iyer *and Abraham* but written with variables available within the ELSA framework:

$$\tau_{coll} = \frac{L_{coll}^3}{S_{eff} u_l} = \frac{C_{col}}{\overline{\rho}\widetilde{\Omega}\sqrt{\frac{2}{3}\widetilde{k}}} \tag{23}$$

If one considers a collision between two droplets characterized by a Weber number We_{coll}. Then, for an initial surface density $\widetilde{\Omega}$, the equilibrium surface density $\Omega^{*}{}_2$ given by conservation of the total energy becomes:

$$\Omega^{*}{}_2 = \widetilde{\Omega} \frac{1 + \dfrac{We^*}{6}}{1 + \dfrac{We_{coll}}{6}}, \tag{24}$$

where We^* is the equilibrium Weber number. Its value has been initially set to $We^* = 15$ [22]. Indeed, this is the approximate value that separates coalescence and separation effect after collision [16]. This model is referred as “Beau” in the following.

From an experimental point of view, binary collision outcomes have been extensively studied, see for instance [16, 26]. Two main parameters are generally used to build a diagram of collision depending on the Weber number of collision together with the impact factor B. Nevertheless, the equilibrium value of the Weber number is not a direct output of these

diagrams. Collision results in new droplets which will experience an extra collision, the missing information is what will be the next Weber of collision after the considered collision. To determine the equilibrium Weber number, another possibility is to find out the distribution of the total energy between the surface energy and the kinetic energy. For instance, at the equilibrium, if the liquid kinetic energy balances the liquid surface energy, then the following relation is obtained:

$$\frac{1}{2} m_l {u_l}^2 = \sigma_l S_l \Rightarrow We^* = \frac{6 u_l^2 \widetilde{Y}_l}{\sigma_l \widetilde{\Omega}} = 12 \tag{25}$$

This model of collision/coalescence effect with this value of We^* has been used in the last version of the ELSA model [4].

However, the formulation of the collision/coalescence source term of Eq.(22) has been postulated but not demonstrated. In this paper, in order to overcome this weakness, a new source term, inspired from Iyer's approach, but with an addition of the contribution due to collision-induced breakup is proposed:

$$\phi_{coal+bup} = (\beta - 2) \overline{\rho} \widetilde{\Omega}^2 \frac{u_l}{3} \tag{26}$$

where β corresponds to the number of droplets formed by the collision between two parent droplets. If β is equal to 1, then this source term is a destruction term of the liquid-gas interface due to coalescence and it is equivalent to the one of Iyer *and Abraham.* If β is greater than 2, the source term becomes a production term of interface due to liquid breakup. From an Eulerian point of view, droplet collisions are considered as a set of collisions and not individually. Accordingly, β does not take necessarily an integer value. Due to collisions the spray evolves in order to reach the equilibrium diameter D_{32}^*. If the current mean diameter

D_{32} is lower than D_{32}^{*} , then coalescence is expected in mean, otherwise collision induced breakup is expected:

$$\begin{cases} \beta \in \left[\max\left(\dfrac{2D_{32}^{3}}{D_{32}^{*\,3}}; 1 \right); 2 \right] & if \quad D_{32} \le D_{32}^{*} \\ \beta \in \left[2; \dfrac{2D_{32}^{3}}{D_{32}^{*\,3}} \right] & if \quad D_{32} > D_{32}^{*} \end{cases} \tag{27}$$

Since the probability density function of the variable β for individual collision is not known, a uniform distribution is used as a first step. Thus :

$$\overline{\beta} = \frac{\beta_{\min} + \beta_{\max}}{2}, \tag{28}$$

where, $[\beta_{\min}, \beta_{\max}]$ describes the prescribed interval of β, see Eq. (26). This model is referred as “New” in the following.

To study the behaviour of each model, a simple test case is put forward. It consists in a spatially homogeneous spray where the kinetic energy of liquid agitation is kept constant. In this case, all parameters of the models are constant. The only variation is due to the evolution of surface density. This can completely be described by a unique Weber number of collision. The previous three models are tested on Fig. 1. Beau’s model and New’s model take into account both the coalescence and the collision induced breakup. Accordingly, after a while they tend to a constant Weber number. At the contrary with the Iyer’s model, the Weber number still increases all along the simulation. Equilibrium is never achieved since only coalescence is considered as far as collisions are concerned. For the three models, the characteristic time is identical but each model leads to a different behaviour during the coalescence phase. It appears that the law proposed by Vallet et *al*. [11] is not in agreement with the other models that are based on droplet interactions. For pure coalescence, the Iyer’s

model and the New's model are identical except for the initial value of 12, proposed by Iyer *and Abraham* [18] that becomes 3 in the New's model.

(Figure 1: about here)

These Eulerian models are compared to their Lagrangian counterpart in the next section.

4 Collision/coalescence: Lagrangian point of view

To model a spray, the traditional Lagrangian approach based on the Discret Droplet Model (DDM) [27], consists in a statistical description of the spray. Stochastic particles or parcels, group of real droplets with similar properties (diameter, temperature, velocities), are tracked in a Lagrangian way inside the domain. To represent accurately a spray, a large particle sample is required. This is one of the major drawbacks of this approach that need additional computational efforts. Unfortunately, collision submodels do not escape to this rule. They are even more expensive in terms of computational resources than the other modeled phenomena. Thus, a compromise between the statistical convergence and the computational resources has to be found.

Two questions are inherent to Lagrangian collision submodels:

1. How to determine the occurrence of collision?
2. How to determine collision outcome?

The first question is merely a numerical and mathematical question. It consists in determining the collision partners and the probability of collision.

Several algorithms exist. A widely known model is without doubt the O'Rourke's model [24] that is based on the kinetic theory through the calculation of a collision frequency.

Unfortunately, this algorithm has several limitations. In particular it can lead to mesh-dependent results and it may have a prohibitive computational cost. Several authors have done proposals to overcome to these problems.

Nordin [28] transposed the collision process in terms of intersection of parcel trajectories. So, droplet collisions have been restricted to parcels whose trajectories intersect at the same time during the time step. To avoid considering all the possible collision partners, even the most unlikely, two criteria related to the parcel displacement have to be respected. Schmidt and Rutland [29] extended the No-Time Counter (NTC) algorithm based on a pre-sampling of collision partners. They used a second independent mesh that is specifically dedicated to the collision process. Li *et al.* [30] proposed an algorithm based on the Smoothed Particle Hydrodynamics (SPH) method. For each parcel, only the closest parcels are considered to be likely to collide. A collision probability defined from the kernel function of the relative distance is then used to determine whether collision occurs.

The second question concerns the collision outcome.

When a collision between two droplets occurs, it is necessary to forecast the collision outcome and to know the post-collision characteristics. The collision outcome depends on the properties of both phases and the intrinsic parameters of the collision (relative velocity, impact parameter and size ratio). In this work, only binary collisions are considered. Several regimes have been observed, such as bounce, permanent coalescence, coalescence followed by a separation (reflexive or stretching) and accompanied or not by new satellite droplets [16]. The boundaries between these regimes are now relatively well-known for low ambient pressures. Recently, a particular attention was devoted to the satellite droplet formation [31, 32] see for instance Fig. 2. This attention is quite legitimate, because satellite droplets formation is very likely to occur in the spray dense region.

(Figure 2: about here)

However, the development of a collision model able to predict the number of satellite droplets along with their sizes and velocities, knowing the medium and liquid properties and the collision characteristics is not fully achieved.

Georjon and Reitz [33] suggested a simple model to translate observations made about the satellite droplets creation for high Weber number. When two droplets collide, a cylinder-shaped liquid mass is induced by the impact, see Fig.2. Then instabilities may propagate, break this liquid ligament and form several satellite droplets. This shattering-collision process takes place beyond a specific value of collision Weber number chosen somewhat arbitrarily, namely about one hundred. Post and Abraham [34] studied collision phenomena for Diesel sprays and proposed a complete model accounting for the above-cited regimes [16] based on experimental results. Because of the computational cost, they simplified the model of Georjon and Reitz for shattering collisions for high Weber values and, they took the effects of local pressure into account: when pressure increases, the domain of bounce regime is enlarged. Hou and Schmidt [35] used the simplification done by Post and Abraham, but considered only the interaction volume of colliding droplets to produce the satellite droplets.

To focus on collision processes, Orme [36, 37] studied the binary droplet collisions in vacuum so that no other process (for instance gas turbulence or secondary break-up) interferes. Similarly, as a test case, collision processes are simulated without taking the action of the gas phase on liquid droplets into account. The droplets are considered ballistic. This avoids the complex interactions between gas and liquid turbulence that depends on turbulent scales and inertial time. The computational domain is cubic box with periodic boundary conditions in all direction. A Lagrangian method is used to follow the stochastic particles, Fig. 3.

(Figure 3: about here)

In this configuration, statistical convergence can be reached by using a sufficiently large sample of stochastic particles. The test case presented here is identical to the one used previously to compare Eulerian models. The configuration is simple enough to allow the O'Rourke's approach [24] to be used, *since only one mesh cell is necessary as far as the Lagrangian simulation is concerned*. To compare with the Eulerian cases, the mean liquid kinetic energy is forced to be constant. Otherwise, due to the coalescence phenomenon, a large part of the initial liquid kinetic energy will be dissipated, see Fig. 4. When coalescence phenomenon occurs, parents droplets have not initially the same velocity. But the resulting drop has only one velocity, hence a part of the initial kinetic energy carried by the parent droplets has vanished. In reality, the dissipated energy creates oscillations within the child droplet. To compensate this sink of liquid kinetic energy, two kinds of forcing have been tested:

1. A linear forcing [38] originally used for the gas phase is applied to the liquid by adding a source term to the droplet velocity equation:

   $$\frac{du_i}{dt} = ... + Au_i \qquad (29)$$

   Where, A is a parameter continuously determined during the computation to compensate exactly the dissipated energy.

2. A complete redistribution of the droplet velocity field at each time step to maintain a prescribed level of liquid kinetic energy.

(Figure 4: about here)

In this study, both forcing techniques give similar results (see Fig. 4). Results presented in the following are obtained using the second method. A consequence of this forcing technique is that it erases any influence of the coalescence on the turbulent liquid field. Accordingly, this effect is not studied here and the present study focuses on collision effects on droplet surface variation.

Initially, the droplets are randomly distributed in the cubic box with the same diameter. Five thousand stochastic particles have been retained to achieve statistical convergence. Characteristics of the test case are summarized in table 1:

(Table 1: about here**)**

Concerning the collision outcomes considered in this study, the coalescence and stretching separation regimes will be taken into account through the Brazier-Smith's correlation [24, 25]. This model is referred as "O'Rourke" in the following. To account for the breakup induced by shattering collision the model of Georjon and Reitz [33] is used and referred as "Georjon". Finally, the most complete model tested in this study is the one proposed by Post and Abraham [34] and is referred as "Post".

Results are presented as a function of the non-dimensional time obtained by using the collision time scale as a reference. A comparison of the three Lagrangian models tested in this work is presented in Fig. 5. O'Rourke model does not account for any collision-induced breakups. Accordingly the Weber number increases all along the simulation. This evolution corresponds

to a continuous increase of the droplet diameter. However, the efficiency of coalescence decreases with time as higher values of the Weber number are reached. Then, the increase rate of the Weber number becomes smaller and smaller, but no equilibrium value is found. Paradoxically, both Georjon and Post models include collisions induced breakup effects and lead to an equilibrium Weber number. The Georjon model behaves similarly to the O'Rourke model at the beginning since droplets are very small and no breakup is expected. Then the simple formulation used in Georjon model to represent breakup due to shattering collision switches on and nearly immediately an equilibrium Weber number ($We^* = 12$) is found. The complete formulation of the Post model takes into account more physical phenomena and balance between coalescence, rebound and breakup is more complex. Thus the differences with the O'Rourke model appear earlier and the transition to the equilibrium Weber number ($We^* = 15$) is smoother. Notice that for both Georjon and Post models, equilibrium Weber number values found in these simulations are not part of the model parameters. A computation of the balance between the various phenomena taken into account by each model is required to determine each corresponding equilibrium Weber number. Values found by Georjon and Post models are different. This is expected since these models are not equivalent. Moreover, these models have been designed with the goal to be in accordance with phenomena observed in binary collisions rather than to fit an experimental value of the equilibrium Weber number. Indeed, such a value has not been measured at our best knowledge and it will not be an easy task. It has to be said that the equilibrium Weber number value depends on the model parameters. Results presented here used standard parameters found in the literature [33, 34]. But some of them are not totally established, for instance Luret et *al*. [39] have shown variation of the equilibrium Weber number when varying the shattering collision Weber number of the Georjon model. Finally, it is interesting to note that both Lagrangian models lead to quite similar equilibrium Weber numbers. That are close to the values proposed in the Eulerian

formulation discussed previously.

(Figure 5: about here)

Fig. 6 presents comparisons of the Eulerian models with the Lagrangian Georjon model. To realize these simulations, the equilibrium Weber number found for the Georjon model has been used $(We^* = 12)$ for both Beau and New Eulerian models. Phenomena taken into account by the Iyer model do not allow the equilibrium to be achieved. Both Eulerian models are able to represent correctly the evolution of the spray as far as the simple Georjon model is concerned. Initially, the New model is closer to the Georjon model than to the Beau model. This is expected because the Eulerian New model has been built considering binary collisions as it is the case in the Lagrangian formulation.

(Figure 6:about here)

Figure 7 shows a comparison of the Eulerian models $(We^* = 15)$ with the more complete Lagrangian Post model. The Eulerian models are not able to reproduce completely the complex behaviour of the Post model. Among the Eulerian models only the New model is able to reproduce the initial behaviour of the Post model. The initial phase is controlled by coalescence phenomenon, so it can be expected that this phase is correctly modeled by the New model. Then, the collision efficiency is decreasing as far as the Post model is concerned. This is not captured in the New model although it is able to reproduce the Georjon model. Comparison of the different assumptions used to derived Georjon and Post models, shows that the rebound phenomena can be the cause of discrepancy between the New model and its Post

counterpart. This could be taken into account through a modification of the probability density function of the parameter β, see Eq. (28).

(Figure 7: about here)

However, in our opinion, before going further in the integration of collisions features occurring between spherical droplets, a missing point in the modelling framework must be addressed.

A common drawback of all collision models is the assumption that collisions occur between spherical droplets whose surface is at rest. But after a collision the droplets are very perturbed and they are animated by strong oscillations, see Fig.2. It can be expected that collisions lead to different behaviour depending on the internal agitation of the colliding droplets. The amount of energy that can be dissipated by the droplet oscillation is shown Fig. 4. Without any forcing procedure, the kinetic energy of the liquid is strongly reduced. This energy becomes internal liquid agitation within the droplets, where it is finally dissipated. To recover a collision between spherical droplets the time needed to dissipate this internal motion must be *shorter* that the collision time. To measure the importance of this phenomenon, the Fig. 2 can be observed. After the collision, the two big droplets oscillate nearly all along their ways out of the measuring zone. Thus the distance covered before the vanishing of the oscillation is about:

$$L_{diss} \approx 20D. \qquad (30)$$

To get spherical collision, the characteristic dissipation time τ_{diss} must be *smaller* than the collision characteristic time of one droplet (τ_{coll}):

$$\tau_{diss} = \frac{L_{diss}}{u_l} > \tau_{coll} \quad \Rightarrow \quad \phi_l < \frac{1}{60}. \tag{31}$$

For this typical case, spherical collisions are limited to sprays where the liquid volume fraction is lower than 2%. Since the collision effects have been expected to be more important for dense spray, it seems legitimate to focus our study on collisions where agitation within the droplet is considered. To do so a new numerical test case is put forward in the next section.

5 A numerical test case to study collision in dense spray

An investigation is conducted on the equilibrium state and its characterization through a Weber number for dense spray. To describe the internal agitation of the droplets, a full DNS for both the gas and the liquid phase has been used and a first test case is put forward as reference.

5.1 Direct Numerical Simulation: code description

Thanks to recent developments, Direct Numerical Simulation can be a powerful tool to study two-phase flows [19, 40]. Indeed, from DNS simulations, statistical information can be collected in the dense zone of the spray where nearly no experimental data are available. Furthermore, these simulations are predictive and quantitative. They have been used already to validate modelling proposal [4]. This is the first objective of the work presented below that

focuses on the liquid-gas interface density, but with a fine description of turbulence effects on the development of the interface.

The numerical method must describe the interface motion precisely, handle jump conditions at the interface without artificial smoothing, and respect mass conservation. Accordingly a 3D code was developed by Ménard et *al.* [19], where interface tracking is performed by a Level Set method. The Ghost Fluid Method is used to capture accurately sharp discontinuities. The Level Set and VOF methods are coupled to ensure mass conservation. A projection method is used to solve the incompressible Navier-Stokes equations that are coupled to a transport equation for level set and VOF functions.

Level Set methods are based on the transport of a continuous function ϕ, which describes the interface between two phases [41, 42]. This function is defined by the algebraic distance between any point of the domain and the interface. The interface is thus described by the 0 level of the Level Set function. Solving a convection equation allows to determine the evolution of the interface in a given velocity field $\mathbf{V}$ [42]:

$$\frac{\partial \phi}{\partial t} + \mathbf{V}.\nabla\phi = 0 \qquad (32)$$

Particular attention must be paid to this transport equation. Problems may arise when the level set method is developed: a high velocity gradient can produce wide spreading and stretching of the level sets, such that ϕ no longer remains a distance function. Thus, a re-distancing algorithm [41] is applied to keep ϕ as the algebraic distance to the interface.

To avoid singularities in the distance function field, a 5^{th} order WENO scheme has been used for convective terms [43]. Temporal derivatives are computed with a third order Runge Kutta scheme.

One advantage of the Level Set method is its ability to represent topological changes both in 2D or 3D geometry quite naturally. Moreover, geometrical information on the interface, such as normal vector $\mathbf{n}$ or curvature κ, are easily obtained through:

$$\mathbf{n} = \frac{\nabla\phi}{|\nabla\phi|} \quad , \quad \kappa(\phi) = \nabla \cdot \mathbf{n} \tag{33}$$

It is well known that numerical computation of equation (32) and a redistance algorithm can generate mass loss in under-resolved regions. This is the main drawback of Level Set methods. However, to improve mass conservation, two main extensions of the method can be developed: namely the Particle Level Set [44] and a coupling between VOF and Level Set [45].

Navier Stokes equations

The Level Set method is coupled with a projection method for the direct numerical simulation of incompressible Navier-Stokes equations expressed as follows:

$$\frac{\partial \mathbf{V}}{\partial t} + (\mathbf{V}\cdot\nabla)\mathbf{V} + \frac{\nabla p}{\rho(\phi)} = \frac{\nabla(2\mu(\phi)\mathbf{D})}{\rho(\phi)} \quad \mathbf{D} = \frac{\nabla\mathbf{V} + \nabla\mathbf{V}^T}{2} \tag{34}$$

$$\nabla \cdot \mathbf{V} = 0 \tag{35}$$

where p is the pressure, ρ and μ are the fluid density and viscosity respectively.

Diffusion is estimated with a 2nd order central scheme. Convective terms are approximated by 5th order WENO scheme to ensure a robust behaviour of the solution. Temporal derivatives are approximated with an Adams Bashforth algorithm.

Poisson equation discretization, with a second order central scheme, leads to a linear system whose matrix is symmetric and positive definite. Various methods can be derived to solve this system. According to different authors [46], the **M**ulti**G**rid method for preconditioning **C**onjugate **G**radient methods (MGCG) combines **I**ncomplete **C**holeski **C**onjugate **G**radient (ICCG) robustness with the multigrid fast convergence rate. Moreover, the MGCG method greatly decreases computational time compared to the ICCG algorithm.

Discontinuities

The interface is defined by two different phases and discontinuities must be taken into account for density, viscosity and pressure. Specific treatment is thus needed to describe the jump conditions numerically.

Two different approaches can be used to represent the above conditions, namely the Continuum Surface Force (CSF) or the Ghost Fluid Method.

To overcome the smoothing effect of the CSF method, the **G**host **F**luid **M**ethod (GFM) has been developed by [47]. The formalism respects jump discontinuities across the interface, and avoids considering an interface thickness. Discretization of discontinuous variables is more accurate, and spurious currents in the velocity field are thus much lower than with CSF methods. This procedure is used to discretize all discontinuous variables, namely density, viscosity, pressure and viscous tensors [48, 49].

In GFM methods, ghost cells are defined on each side of the interface [49, 50] and appropriate numerical schemes are applied for jump conditions. As defined above, the interface is characterized through the distance function, and jump conditions are extrapolated on some nodes on each side of the interface. Following the jump conditions, the discontinued functions are extended continuously and then the derivatives are estimated.

More details can be found in [50] on implementing the Ghost Fluid Method to solve the Poisson equation with discontinuous coefficients and obtain solution with jump condition.

Level Set-VOF coupling

A lot of liquid parcels (droplets, ligaments, liquid sheets…) are generated in the primary break up of a jet and the coupling between the VOF and the Level Set methods is necessary. The main idea is to take advantage of each strategy: mass conservation from the VOF and fine description of the interface with the level set and Ghost fluid methods. The numerical method used here is quite similar to the CLSVOF of Sussman and Puckett [19, 45]. Tin our approach, the main differences with the CLSVOF lie in the fact that the initial redistancing algorithm is conserved. In addition, the reconstruction technique is modified to define the interface in a cell thanks to the Level Set position.

5.2 Test case and preliminary results

To compute the whole interactions between the liquid and the gas phases, the DNS approach described above is used in the following. Similarly to the previous test cases used for Eulerian and Lagrangian simulations, a homogeneous spray is considered. The computational domain is a cubic box with periodic boundary conditions in all directions. Since all scales of the two phase flow are computed, the numerical effort is more intensive than for the previous test cases. As a consequence it is difficult to achieve statistical convergence by volume averaging only. Thus, time averaging is also considered. To do so, a stationary behaviour is required especially for the turbulent kinetic energy. Consequently, to compensate the continuous dissipation of the kinetic energy, the turbulence has to be forced. For single phase flows [51]

and even dispersed two phase flows [52] spectral methods are generally used to inject kinetic energy in the largest scales of the flow. However, the spectral behaviour of two phase flows, which is studied here, is not well known. Accordingly, a simple linear forcing method is applied here to the liquid-gas mixture to limit artificial hypothesis. Recently, Rosales and Meneveau [38] have shown that this approach is comparable to spectral methods in the framework of single phase flows.

Thanks to this method, the mean turbulent kinetic energy reaches a targeted level. The linear forcing consists in adding one source term to the velocity equations similarly to Eq. 29. This source term is proportional to the velocity fluctuations through a parameter A. This parameter is continuously adjusting to sustain the prescribed level of turbulent kinetic energy. Figure 8 represents the temporal evolution of the turbulent kinetic energy considering the complete mixture: gas and liquid.

Initially, eight droplets are dispatched in the cubic box, one at each corner. The initial droplet diameter is determined by a given liquid volume fraction. An initial rotational velocity is set for each droplet; the velocity magnitude is in accordance to the prescribed level of kinetic energy. The linear forcing of the turbulence is initially deactivated. During the first phase, starting from instable conditions, the flow becomes turbulent and relaxes gently. This leads to a decrease off the turbulent kinetic energy at the beginning of the simulation. Then, the forcing method is activated and the turbulence intensity reaches its prescribed level, see Fig. 8.

(Figure 8: about here)

(**Table 2:** About here)

Properties of the simulation are summarized in table 2. After initialisation, the mean characteristics of the flow reach a stable state. Pictures of the liquid interface during a collision are shown in Fig. 9. The collision takes place in the bottom left corner. The figure represents successive images of the liquid surface from left to right and from top to bottom. The time interval between two consecutive images is 1.7 ms. At the end of this sequence a new collision is observed for the same parcel of liquid on the bottom right corner. Clearly there is not enough time between the two collisions to dissipate the agitation induced by the first collision. Different liquid structures, more or less tortuous, are observed. The interactions between the turbulent gas motion and the liquid parcel but also between the liquid parcels themselves lead to non spherical parcels of liquid. Note that the two phase flow is relatively dilute since the liquid volume fraction is only 5% (but above the limit of 2% found previously in Eq. (31) to get a regime of spherical collisions). Only the smallest parcels show a spherical behaviour, but they represent clearly a very small part of the total amount of liquid. Most collisions occur between parcels of liquid that cannot be considered as droplets.

(Figure 9: about here)

Accordingly, the droplet diameter that is generally used to build the Weber number of collision cannot be chosen anymore. Coming back to the formulation proposed in the context of Eulerian methods, the Weber number of collision writes:

$$We = 12\frac{\tilde{Y}_l \frac{1}{2}\overline{u_l}^2}{\sigma_l \tilde{\Omega}} = \frac{12}{3}\frac{\tilde{Y}_l \bar{k}_l}{\sigma_l \tilde{\Omega}} \qquad (36)$$

The relative velocity between liquid parcels u_l has been expressed in terms of turbulent kinetic energy in the liquid phase, $\bar{k}_l$ similarly to Eq. (18). The modelling constant appearing

in the equation is set to unity. The evolution of the Weber number of collision is represented in Fig.10. The dashed line represents the instantaneous evolution obtained by considering the whole computational domain. The solid line represents the collision Weber number averaged over time.

After the initialisation phase, the Weber number of collision oscillates around its equilibrium value. The mean value found for this case is about $We^* = 3.5$. This value is not identical to those previously used for Eulerian or Lagrangian models ($12 < We^* < 15$). Before stating about the accuracy of the equilibrium Weber value obtained by DNS, some issues have do be addressed. Concerning the influence of the mesh, a test case using a grid of 64x64x64 mesh cells has been tested and gives similar results. A larger box is expected to get a proper statistical convergence over the computational model to study also the evolution of the Weber number. It is also important to note that the periodic boundary condition imposes a scale of symmetry. To get more universal results the distance between periodic conditions must be larger than the other scale of the flow, in particular larger than the free mean path of collision. As a consequence very dilute sprays should be difficult to study using this approach. Despite these drawbacks the DNS approach brings some light on collision processes for spray not completely dispersed. It is important to stress that sprays characterized by a liquid volume fraction of few percents are sprays where collisions are prevalent. The present simulation demonstrates the importance of collisions between non spherical droplets. More data are necessary to characterize this phenomenon. The present work shows that comprehensive results can be obtained thanks to the complete DNS of two phase flows.

(Figure 10: about here)

6 Conclusion

Based on recent progresses in the field of atomisation modelling, it appears necessary to study collisions in moderately dense flows. Special atomisation models able to compute realistically the dense zone of the spray have been developed since the pioneering work of Vallet et al. [11, 17]. A difficult point concerns the representation of the collision processes, in particular on the evolution of the liquid-gas surface density. A description of the ELSA model is presented to show the part of the model where collisions are expected to play a role. Other formulations of the Eulerian models dedicated to collisions are compared and the importance of the equilibrium Weber number has been demonstrated. Classical models of atomisation have been developed in the context of Lagrangian formulations. These formulations have been used as reference to test the ability of Eulerian approaches to address the collision phenomena, in particular coalescence and collision induced breakup. Eulerian models are able to reproduce correctly the behaviour of simple Lagrangian models of collision [33]. For a more detailed Lagrangian model [34], the present Eulerian model fails to reproduce the total complexity of the phenomena. This study shows also that current collision modelling leads to equilibrium Weber number values ranging between 12 and 15. Before developing more detailed Eulerian models of collision, it is outlined that current models consider only collisions between spherical droplets. Experimental observations show that the droplets issued from a collision are subject to a significant internal agitation, which can play a key role to determine the outcome of the next collision. When looking at an experimental observation of a collision, it appears that the droplet oscillations need a long characteristic time to be dissipated. For this particular test case, a regime of collision between spherical droplets with no internal agitation can be considered only for spray with liquid volume fraction lower than 2%. To study the influence of non spherical collision in moderately dense spray, a numerical test case based on complete DNS of the spray has been put forward. Despite some drawbacks discussed in this paper, the behaviour of the liquid-gas interface for a spray undergoing

collisions with stationary turbulent conditions has been studied. As expected, the spray is mainly composed of non spherical droplets. Collision behaviour looks different to those encountered when considering collisions of spherical droplets. A first equilibrium Weber number of collisions has been determined with a value of 3.5. This value differs from those found previously for Eulerian and Lagrangian models. This may be an effect of non spherical collisions, but DNS test cases must be firmly established to assess this equilibrium Weber value definitively. Using a complete DNS lets foresee interesting future prospects to better understand turbulent two-phase flows. In particular turbulence and collision effects on the topology of the liquid-gas interface will be studied soon. This in complement to experiments on non spherical droplet collision is certainly one of the most interesting perspectives of this work.

7 Acknowledgment

This work was financially supported by PSA Peugeot Citröen. All the authors would like to thank them for their continuous support and their trust. Particular thanks are given to Pr. Brenn for his help. The authors thank the CRIHAN and CINES for CPU time and assistance.

8 Nomenclature

A	Turbulence forcing parameter
D_{32}	Sauter mean diameter
f	*Frequency per unit of volume*
L	Characteristic length scale
k	Turbulent kinetic energy
$\dot{m}_{v,ELSA}$	Vaporisation rate per unit of liquid surface
N_d	Droplet number per unit of volume
n	Vector normal to the liquid surface κ
Oh	Ohnesorg number
P	Pressure
Sc	Schmidt number
S_{eff}	Cross-section of collision
u	Velocity
V	Velocity field
Y	Mass fraction
We	Weber number

Greek Symbols

ϕ_l	Liquid volume fraction
ϕ	Distance function
β	Number of droplet issued of a binary collision
κ	Curvature of the surface
Ω	Liquid surface density per unit of mass
Ψ	Repartition function of surface density source terms between dense and dilute zone
η_{coll}	Coalescence efficiency
ρ	Density
Σ	Liquid surface density per unit of volume
σ	Surface tension coefficient
μ	Dynamic viscosity
τ	Characteristic time scale

Subscripts

coll	Collision
diss	Dissipation of droplet internal agitation
g	Gas
l	Liquid
t	Turbulent

Superscripts

*	Equilibrium value

9 Reference

1. C.K. Sarre, S.C. Kong, and R.D. Reitz, *Modeling the effects of injector nozzle geometry on diesel sprays.* SAE Technical Papers, 1999(1999-01-0912).
2. T.F. Su, M.A. Patterson, R.D. Reitz, and P.V. Farrell, *Experimental and numerical studies of high-pressure multiple injection sprays.* SAE Technical Papers, 1996(960861).
3. C.S. Lee, K.H. Lee, R.D. Reitz, and S.W. Park, *Effect of split injection on the macroscopic development and atomization characteristics of a diesel spray injected through a common-rail system.* Atomization and Sprays, 2006. 16: p. 543-562.
4. R. Lebas, T. Menard, P.A. Beau, A. Berlemont, and F.X. Demoulin, *Numerical simulation of primary break-up and atomization: DNS and modelling study.* International Journal of Multiphase Flow, 2009. 35(3): p. 247-260.
5. W. Cai, C.F. Powell, Y. Yue, S. Narayanan, J. Wang, M.W. Tate, M.J. Renzi, A. Ercan, E. Fontes, and S.M. Gruner, *Quantitative analysis of highly transient fuel sprays by time-resolved x-radiography.* Applied Physics Letters, 2003. 83(8): p. 1671-1673.
6. H. Chaves, C. Kirmse, and F. Obermeier, *Velocity measurements of dense diesel fuel sprays in dense air.* Atomization and Sprays, 2004. 14(6): p. 589-609.
7. J.B. Blaisot and J. Yon, *Droplet size and morphology characterization for dense sprays by image processing: application to the Diesel spray.* Experiments in Fluids, 2005. V39(6): p. 977-994.
8. G. Blokkeel, R. Borghi, and B. Barbeau, *A 3d Eulerian model to improve the primary breakup of atomizing jet.* SAE Technical Papers, 2003. 2003-01-0005.
9. P.A. Beau, M. Funk, R. Lebas, and F.X. Demoulin, *Applying quasi-multiphase model to simulate atomization processes in Diesel engines: Modeling of the slip velocity.* SAE Technical Papers, 2005. 2005-01-0220
10. R. Lebas, G. Blokkeel, P.A. Beau, and F.X. Demoulin, *Coupling vaporization model with the Eulerian-Lagrangian Spray Atomization (ELSA) model in Diesel engine conditions.* SAE Technical Papers, 2005. 2005-01-0213
11. A. Vallet, A.A. Burluka, and R. Borghi, *Development of a Eulerian model for the "Atomization" of a liquid jet.* Atomization and Sprays, 2001. 11(6): p. 619-642.
12. F.-X. Demoulin, P.-A. Beau, G. Blokkeel, A. Mura, and R. Borghi, *A new model for turbulent flows with large density fluctuations: Application to liquid atomization.* Atomization and Sprays, 2007. 17(4): p. 315-345.
13. C. Morel, *On the surface equations in two-phase flows and reacting single-phase flows.* International Journal of Multiphase Flow, 2007. 33(10): p. 1045-1073.
14. V. Iyer and J. Abraham, *Two-fluid modeling of spray penetration and dispersion under diesel engine conditions.* Atomization and Sprays, 2005. 15(3): p. 249-269.
15. J. Chesnel, J. Reveillon, F.X. Demoulin, and T. Ménard, *Subgrid modeling of liquid atomization*, in *ILASS Europe*. 2008: Como Lake, Italy.
16. J. Qian and C.K. Law, *Regimes of coalescence and separation in droplet collision.* Journal of Fluid Mechanics, 1997. 331: p. 59-80.
17. A. Vallet and R. Borghi, *Modélisation Eulerienne de L'atomisation d'un Jet Liquide.* C. R. Acad. Sci., Paris, Sér. II b, 1999. 327: p. 1015–1020.
18. V. Iyer and J. Abraham, *An evaluation of a two-fluid Eulerian-liquid Eulerian-gas model for diesel sprays.* Journal of Fluids Engineering, Transactions of the ASME, 2003. 125(4): p. 660-669.

19. T. Menard, S. Tanguy, and A. Berlemont, *Coupling level set/VOF/ghost fluid methods: Validation and application to 3D simulation of the primary break-up of a liquid jet.* International Journal of Multiphase Flow, 2007. 33(5): p. 510-524.
20. B. Abramzon and W.A. Sirignano, *Droplet vaporization model for spray combustion calculations.* International Journal of Heat and Mass Transfer, 1989. 32(9): p. 1605-1618.
21. W.A. Sirignano, *Fluid Dynamics and Transport of Droplets and Sprays* 1999, Cambridge, United Kingdom: Cambridge University Press
22. P.A. Beau and F.X. Demoulin, *A multiphase flow approach and a single-phase flow approach in the context of a Euler model for primary break-up*, in *ILASS Europe*. 2004: Nottingham (UK).
23. M. Pilch and C.A. Erdman, *Use of breakup time data and velocity history data to predict the maximum size of stable fragments for acceleration-induced breakup of a liquid drop.* International Journal of Multiphase Flow, 1987. 13(6): p. 741-757.
24. P.J. O'Rourke and F.V. Bracco, *Modelling of drop interactions in thick sprays and a comparison with experiments.* The Institution of Mechanical Engineers, 1980(9).
25. P.R. Brazier-Smith, S.G. Jennings, and J. Latham, Vol., *The interaction of falling water drops: coalescence.* Proceedings of the Royal Society of London A, 1972. 326: p. 393-408.
26. M. Orme, *Experiments on droplets collisions, bounce, coalescence and disruption.* Progress in Energy and Combustion Science, 1997. 23: p. 063-079.
27. J.K. Dukowicz, *A particle-fluid numerical model for liquid sprays.* Journal of Computational Physics, 1980. 35(2): p. 229-253.
28. N. Nordin, *Complex chemistry modeling of Diesel spray combustion*. 2000, Chalmers University of Technology, Sweden.
29. D.P. Schmidt and C.J. Rutland, *A new droplet collision algorithm. Journal of Computational Physics.* 2000. 164: p. 62-80.
30. Q. Li, T. Cai, G. He, and C. Hu, *Droplet collision and coalescence model* Applied Mathematics and Mechanics, 2006. 27: p. 67-73.
31. G. Brenn and V. Kolobaric, *Satellite droplet formation by unstable binary drop collisions.* Physics of Fluids, 2006. 18(8): p. 087101.
32. G. Brenn, D. Valkovska, and K.D. Danov, *The formation of satellite droplets by unstable binary drop collisions.* Physics of Fluids, 2003. 13: p. 2463-2477.
33. T.L. Georjon and R.D. Reitz, *A drop-shattering collision model for multidimensional spray computations.* Atomization and Sprays, 1999. 9: p. 231-254.
34. S.L. Post and J. Abraham, *Modeling the outcome of drop-drop collisions in Diesel Sprays.* International Journal of Multiphase Flow, 2002. 28: p. 997-1019.
35. S. Hou and D.P. Schmidt, *Adaptive collision meshing and satellite droplet formation in spray simulations.* International Journal of Multiphase Flow, 2006. 32(8): p. 935-956.
36. M. Orme and K.D. Willis, *Experiments on the dynamics of droplet collisions in a vacuum.* Experiments in Fluids, 2000. 29: p. 347-358.
37. M. Orme and K.D. Willis, *Binary droplets collisions on a vacuum environment: an experimental investigation of the role of viscosity.* Experiments in Fluids, 2003. 34: p. 028-041.
38. C. Rosales and C. Meneveau, *Linear forcing in numerical simulations of isotropic turbulence: Physical space Implementations and convergence properties.* Physics of Fluids, 2005. 17(9): p. 095106.

39. G. Luret, R. Lebas, G. Blokkeel, A. Berlemont, and F.X. Demoulin, *Study of collision/coalescence effects with the ELSA model for Diesel injection*, in *International Conference on Multiphase Flow*. 2007: Leipzig, Germany.
40. S. Tanguy and A. Berlemont, *Application of a level set method for simulation of droplet collisions.* International Journal of Multiphase Flow, 2005. 31(9): p. 1015-1035.
41. M. Sussman, E. Fatemi, P. Smereka, and S. Osher, *Improved level set method for incompressible two-phase flows.* Computers & Fluids, 1998. 27(5-6): p. 663-680.
42. J.A. Sethian, *Level Set Methods and Fast Marching Methods: Evolving interface in computational geometry, fluid mechanics, computer vision and materal science* 1999: Cambridge University Press
43. G.S. Jiang and C.W. Shu, *Efficient implementation of weighted essentially non-oscillatory schemes.* Journal of Computational Physics, 1996. 126: p. 202-228.
44. D. Enright, R. Fedkiw, J. Ferziger, and I. Mitchell, *A Hybrid Particle Level Set Method for Improved Interface Capturing.* Journal of Computational Physics, 2002. 183(1): p. 83-116.
45. M. Sussman and E.G. Puckett, *A Coupled Level Set and Volume-of-Fluid Method for Computing 3D and Axisymmetric Incompressible Two-Phase Flows.* Journal of Computational Physics, 2000. 162(2): p. 301-337.
46. O. Tatebe, *The multigrid preconditioned conjugate gradient method*. 1996, University of Tokyo.
47. R. Fedkiw, T. Aslam, B. Merriman, and S. Osher, *A non-oscillatory eulerian approach to interfaces in multimaterial flows (the ghost fluid method).* Journal of Computational Physics, 1999. 152: p. 457-492.
48. S. Tanguy, *Développement d'une méthode de suivi d'interface. Applications aux écoulements diphasiques*. 2004, PhD thesis of the University of Rouen.
49. M. Kang, R.P. Fedkiw, and X.D. Liu, *A boundary condition capturing method for multiphase incompressible flow.* Journal of Scientific Computing, 2000. 15(3): p. 323-360.
50. X.-D. Liu, R.P. Fedkiw, and M. Kang, *A Boundary Condition Capturing Method for Poisson's Equation on Irregular Domains.* Journal of Computational Physics, 2000. 160(1): p. 151-178.
51. L. Guichard, J. Reveillon, and R. Hauguel, *Direct numerical simulation of statistically stationary one- and two-phase turbulent combustion: A turbulent injection procedure.* Flow, Turbulence and Combustion, 2004. 73(2): p. 133-167.
52. J. Reveillon and F.-X. Demoulin, *Effects of the preferential segregation of droplets on evaporation and turbulent mixing.* Journal of Fluid Mechanics, 2007. 583: p. 273-302.

Liquid volume fraction	0.1
Mean Sauter diameter (m)	8.9e-05
Liquid kinetic energy ($m^2.s^{-2}$)	1.19
Box Length (m)	0.001
Liquid density ($kg.m^{-3}$)	991
Liquid tension surface ($kg.s^{-2}$)	0.07

Table 1: Test case characteristics.

Domain sizes (m^3)	0.01^3
Grid	128^3
Prescribed turbulent kinetic energy ($m^2.s^{-2}$)	0.08
Liquid volume fraction	0.05
Gas density ($kg.m^{-3}$)	25
Liquid density ($kg.m^{-3}$)	753.6
Liquid surface tension ($N.m^{-1}$)	0.0222

Table 2: Test case characteristics.

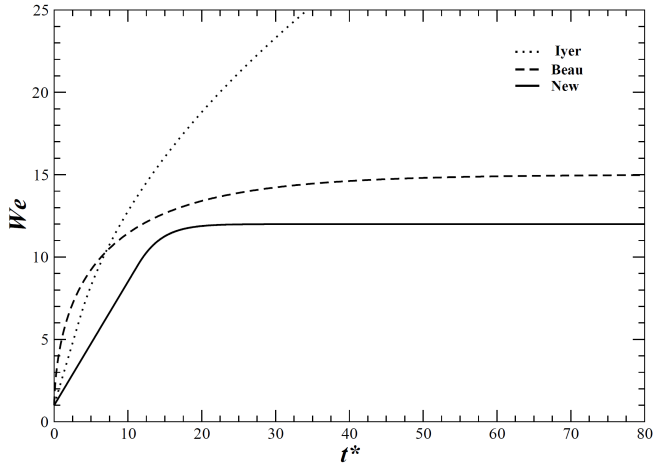

Figure 1: Temporal evolution of Weber of collision for the three different Eulerian models.

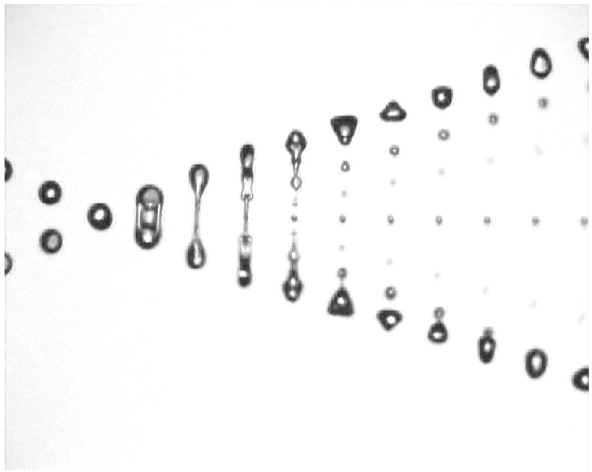

Figure 2: Satellite droplet formation by binary drop collisions, [31]

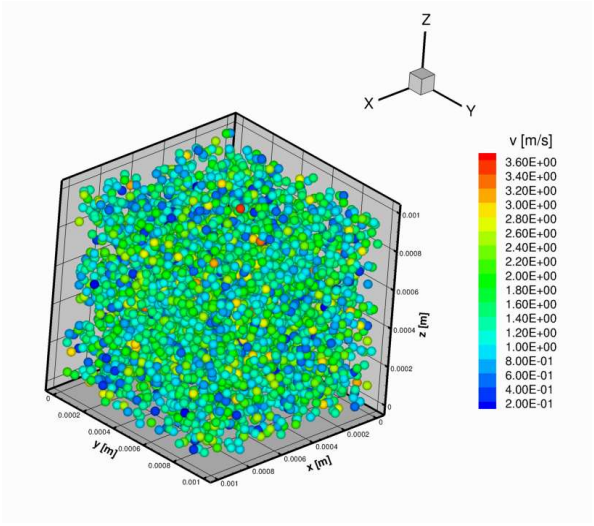

Figure 3: Periodic box: Initial field, droplet colorized by the magnitude of their velocity ($m.s^{-1}$).

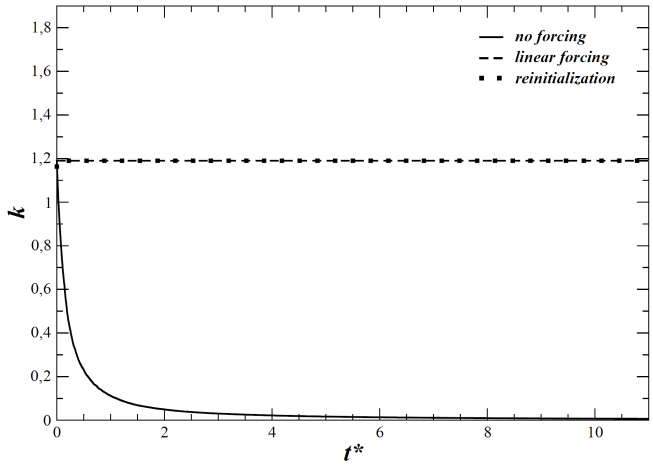

Figure 4: Temporal evolution of the liquid kinetic energy with or without forcing.

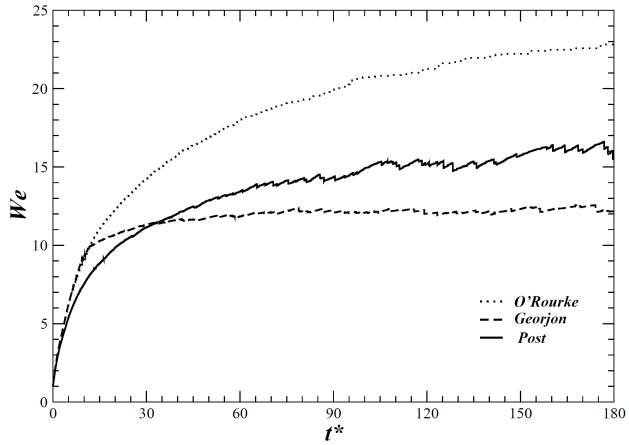

Figure 5: Temporal evolution of the collision Weber number for the three Lagrangian models: O'Rourke, Georjeon and Post.

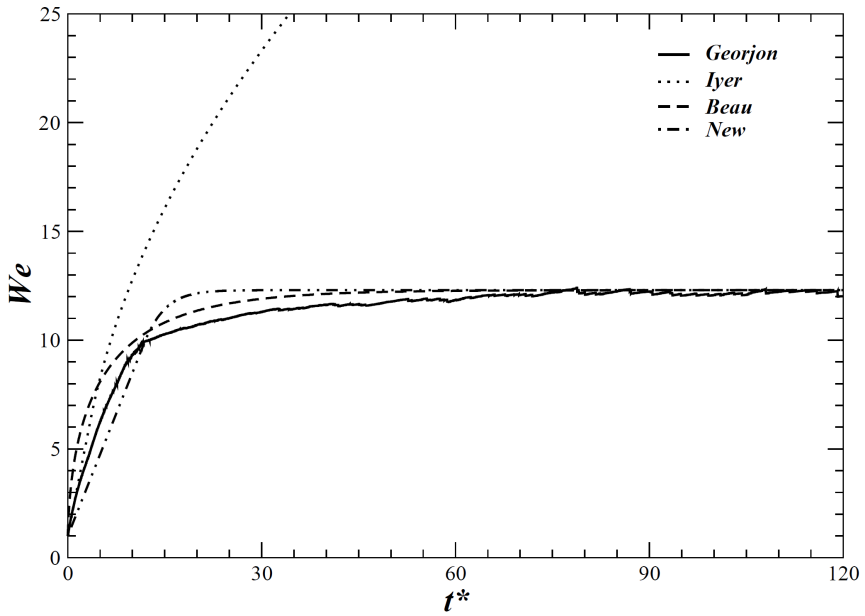

Figure 6: Temporal evolution of the collision Weber number for the three Eulerian models: Iyer, Beau, New compared with the Lagrangian model Georjeon

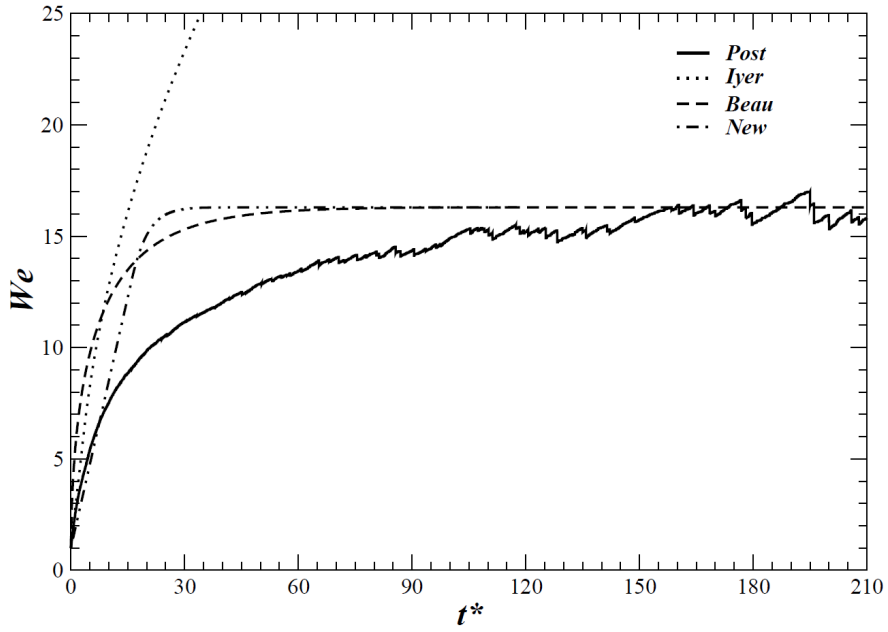

Figure 7: Temporal evolution of the collision Weber number for the three Eulerian models: Iyer, Beau, New compared with the Lagrangian model Post

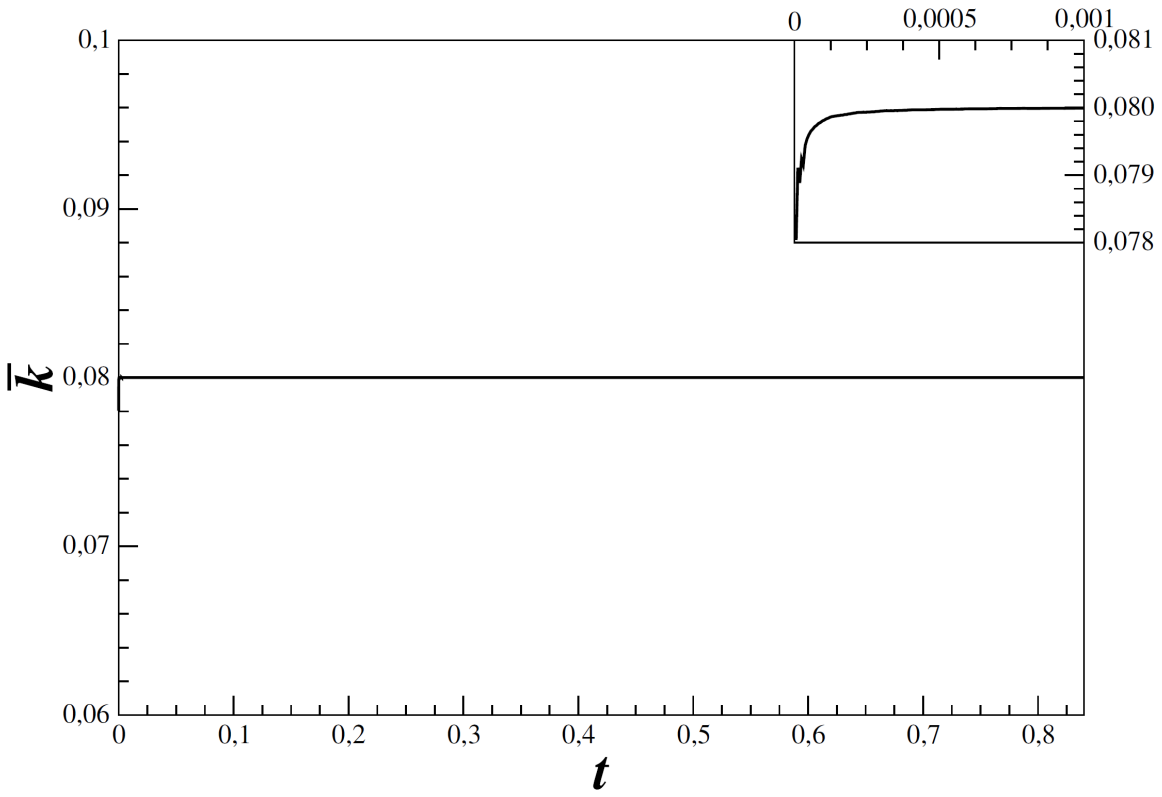

Figure 8: Temporal evolution of the turbulent kinetic energy.

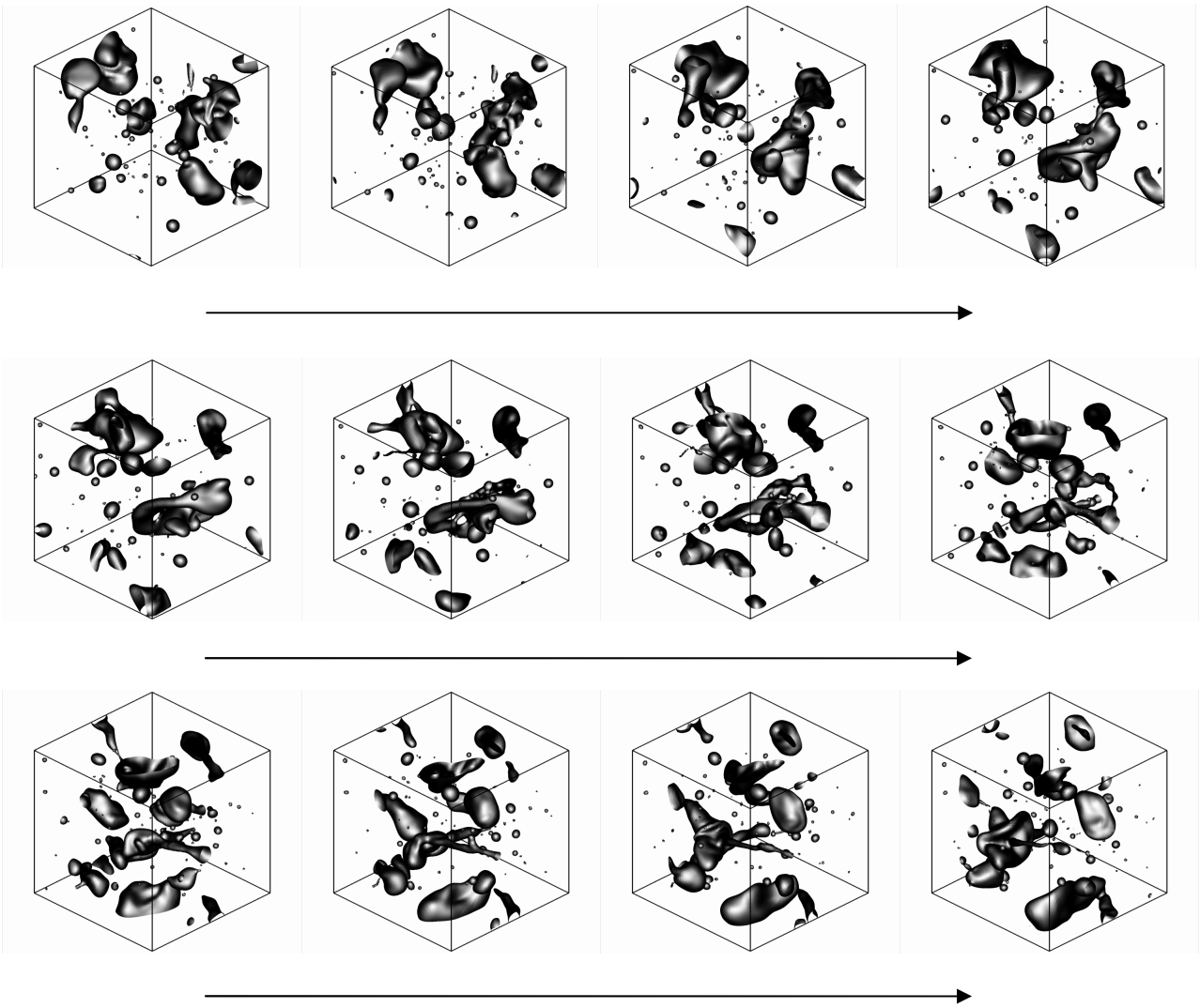

Figure 9: Surface evolution during collision process, one frame every 1.7ms, *the computational domain volume is* $V=0.01^3[m^3]$.

.

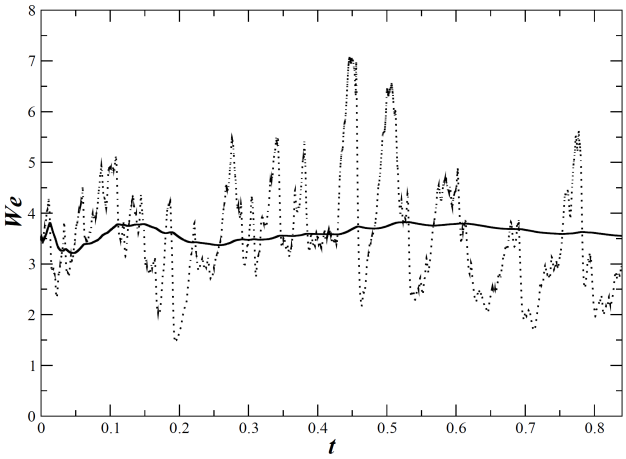

Figure 10: Temporal evolution of the collision Weber number.